BULLETIN OF STOMATOLOGY AND MAXILLOFACIAL SURGERY
Volume 21, Issue 9

DOI:10.58240/1829006X-2025.21.9-227

ORIGINAL RESEARCH

EXPLORING BETANIN'S ANTIANGIOGENIC AND PROHEALING EFFECTS IN DENTAL TISSUE REGENERATION EVIDENCE FROM ZEBRAFISH AND CAM MODELS

Taneesha Sood, Karthik Ganesh Mohanraj, Taniya Mary Martin, Umar Dawood. J,Meenakshi Sundaram Kishore Kumar*

Department of Anatomy, Zebrafish Facility, Saveetha Dental College, Saveetha Institute of Medical and Technical Sciences (SIMATS), Saveetha University, Chennai-600077, Tamil Nadu, India

***Corresponding author:** Meenakshi Sundaram Kishore Kumar Department of Anatomy, Zebrafish Facility, Saveetha Dental College, Saveetha Institute of Medical and Technical Sciences (SIMATS), Saveetha University, Chennai-600077, Tamil Nadu, India meenakshisundaram.sdc@saveetha.com

Received: *Aug 25, 2025;* ***Accepted:*** *Sep, 2025;* ***Published:*** *Oct, 5,2025*

ABSTRACT

Background: Regeneration of dental and periodontal tissues requires a coordinated interplay between angiogenesis, inflammation control, and extracellular matrix remodelling. Tissue repair can be impeded by excessive or unregulated vascularization and inflammation. Betanin, a natural pigment derived from beetroot, has shown promising antioxidant, anti-inflammatory, and wound-healing effects. However, its role in modulating angiogenesis and promoting regeneration in dental tissues is yet to be explored.

Objectives: To investigate the antiangiogenic and prohealing potential of betanin in dental tissue regeneration using zebrafish fin regeneration and chick chorioallantoic membrane (CAM) models, and to elucidate its effects on the expression of key genes associated with angiogenesis, inflammation, and tissue remodelling.

Methods: Zebrafish were subjected to caudal fin amputation and treated with betanin at concentrations of 5 and 10 µg/mL for 7 days. Fin regrowth was assessed macroscopically and histologically. In parallel, CAM assays were performed by applying betanin (1, 5, 10, 25, 50 µg/egg) on day 7 of incubation. After 48 hours, branching, vascular density, avascular zone formation, and vessel count were quantified. Gene expression analysis of BMP2, FGF2, VEGF-A, MMP9, HIF-1α, IL-6, and TNF-α was conducted using qRT-PCR on harvested fin and CAM tissues.

Results: Fin regeneration was enhanced by Betanin therapy in zebrafish, with improved tissue architecture and vascular organization. In CAM assays, higher concentrations of betanin (25 and 50 µg) significantly reduced blood vessel branching and density while increasing avascular zone size, indicating a concentration-dependent antiangiogenic effect. Gene expression analysis revealed upregulation of regenerative markers BMP2 and FGF2, and downregulation of VEGF-A, HIF-1α, MMP9, IL-6, and TNF-α, which suggested betanin promotes healing while inhibiting excessive inflammation and angiogenesis.

Conclusion: Betanin exhibits dual properties entailing pro-regenerative and antiangiogenic effects by enhancing tissue repair and regulating angiogenic and inflammatory pathways. These findings support its potential application in dental tissue engineering and wound healing formulations.

Keywords: Betanin, angiogenesis, zebrafish, CAM assay, dental regeneration, VEGF-A, BMP2, TNF-α, inflammation, wound healing

INTRODUCTION

Tissue regeneration, particularly in the context of dental and craniofacial injuries, is a complex physiological process involving the coordinated interaction of cells, growth factors, and signalling pathways to restore both form and function[1]. Periodontal tissues and alveolar bone are highly vascularized and heavily dependent on angiogenesis and inflammatory modulation for effective regeneration. The clinical management of periodontal diseases and post-surgical healing in dental treatments still faces significant challenges, including prolonged inflammation, poor vascularization, and incomplete tissue regeneration. In this regard, identifying natural bioactive compounds that promote wound healing while simultaneously modulating angiogenesis and inflammation offers an exciting therapeutic avenue[2].

One such promising compound is betanin, a water-soluble betanin pigment predominantly found in beetroot (*Beta vulgaris*). It is known for its vibrant red-violet color and potent antioxidant capacity, betanin has drawn increasing interest in biomedical applications, including cancer prevention, oxidative stress regulation, and wound healing[3]. Betanin's role in tissue regeneration has been uncovered in recent research; however, its specific effects on dental tissue repair and angiogenesis remain largely unexplored. In the context of dental regenerative therapy, where vascular support and inflammatory control are crucial, understanding betanin's dual effects—both prohealing and antiangiogenic—may open new paradigms for clinical application[4].

A critical role in wound healing is played through angiogenesis by supplying oxygen, nutrients, and immune cells to the regenerating tissue. Vascular Endothelial Growth Factor A (VEGF-A) is a central regulator of angiogenesis, and its expression is tightly modulated during tissue injury and repair. While physiological angiogenesis is essential for healing, excessive or dysregulated angiogenic signalling can contribute to chronic inflammation, granulation tissue overgrowth, and fibrotic outcomes—especially in periodontal environments. Therefore, a balanced modulation of VEGF-A and its downstream signals is key to achieving optimal healing.In addition to VEGF-A, Fibroblast Growth Factor 2 (FGF2) is a potent mitogen involved in both angiogenesis and fibroblast proliferation. FGF2 plays a dual role in promoting epithelialization and matrix remodelling, but its overactivation has also been associated with aberrant tissue repair. Hence, regulating FGF2 expression can ensure proper tissue regeneration without promoting pathological angiogenesis[5,6].

Bone Morphogenetic Protein 2 (BMP2) is another gene of interest in wound healing, which is fundamental to osteogenic differentiation and mineralization. BMP2 is a well-known target in dental bone regeneration strategies due to its ability to activate signalling cascades that promote the differentiation of mesenchymal stem cells into osteoblasts. Modulating BMP2 expression in the presence of bioactive compounds like betanin may reveal insights into its osteoinductive or regenerative potential in dental tissues.Another crucial component of the healing process is Inflammation. Acute inflammation aids in microbial clearance and tissue debridement, but chronic inflammation impairs regenerative efficiency[7]. Key inflammatory cytokines such as Tumor Necrosis Factor-alpha (TNF-α) and Interleukin-6 (IL-6) are upregulated in response to injury and microbial insults. While they are essential for initiating the repair response, their sustained expression often leads to tissue degradation and fibrosis. A controlled downregulation of these cytokines has been associated with improved tissue integrity and accelerated healing. Betanin, as a known anti-inflammatory agent, may exert beneficial effects by modulating the expression of TNF-α and IL-6, reducing inflammatory burden in dental tissues[8].

Matrix Metalloproteinase-9 (MMP9) is another pivotal player in the remodelling of the extracellular matrix (ECM) during wound healing. MMP9 facilitates cell migration, matrix turnover, and angiogenesis. However, elevated MMP9 levels can also degrade essential ECM components, contributing to tissue destruction in periodontal disease. Therefore, It is important to prevent excessive breakdown of the regenerating matrix by controlling MMP9 activity. Natural compounds like betanin may provide a regulatory influence on MMP9 expression, offering both structural preservation and regenerative support.

Hypoxia-inducible factor 1-alpha (HIF-1α) is a transcription factor stabilized under hypoxic conditions—common during early wound healing and angiogenesis. It upregulates downstream genes including VEGF-A and is essential for initiating vascular responses during tissue injury. However, its sustained activation may favor excessive or pathological angiogenesis. Modulating HIF-1α levels is, therefore, critical for balancing oxygen supply, tissue oxygenation, and new vessel formation. The antioxidant potential of betanin might mitigate hypoxia-induced oxidative stress and modulate HIF-1α activity, contributing to a more regulated healing response[9].

In this study, we investigate the therapeutic role of betanin in dental tissue regeneration using two well-established biological models: the zebrafish caudal fin regeneration model and the chick chorioallantoic membrane (CAM) assay. Zebrafish are a widely used vertebrate model for studying tissue regeneration due to their remarkable ability to regrow amputated fins and their transparent, externally developing embryos, which allow real-time visualization of vascular and regenerative processes. The zebrafish model provides an excellent system for evaluating both osteogenic signalling and tissue regrowth in response to betanin treatment[10,11].The CAM assay, on the other hand, offers a robust in vivo platform to assess angiogenesis and inflammatory modulation. Due to its rich vascular network and ease of access, the CAM membrane allows for the direct application of test compounds and real-time monitoring of blood vessel formation, branching, and regression. The CAM assay when used alongside the zebrafish model adds translational relevance by providing antiangiogenic insights in a mammalian-resembling vasculature[12].

Through these models, we aim to explore how betanin modulates the expression of critical genes involved in tissue regeneration (BMP2, FGF2), angiogenesis (VEGF-A, HIF-1α), matrix remodelling (MMP9), and inflammation (IL-6, TNF-α). Our hypothesis is that betanin promotes a balanced healing environment by upregulating pro-regenerative markers (e.g., BMP2) while downregulating proangiogenic and pro-inflammatory mediators (e.g., VEGF-A, IL-6, TNF-α), thereby facilitating efficient yet controlled tissue regeneration. Understanding the gene-level influence of betanin on dental and periodontal healing processes may pave the way for its application as a bioactive compound in oral care formulations, regenerative dental biomaterials, and post-surgical wound management[13,14].

Moreover, this study responds to the growing need for plant-based, biocompatible alternatives to synthetic drugs in dentistry. The use of growth factors, scaffolds, or synthetic drugs are often involved in current regenerative therapies that may carry risks of adverse reactions, high costs, or regulatory barriers. Natural molecules like betanin offer an eco-friendly, affordable, and multifunctional alternative that can address multiple facets of tissue repair—antioxidant protection, inflammatory regulation, vascular modulation, and bone regeneration. Therefore, understanding the molecular mechanisms underlying betanin's biological activity can support its integration into future clinical and dental regenerative strategies[15].

2 MATERIALS AND METHODS

2.1 Chemicals and Reagents

Betanin (≥98% purity), a natural betanin pigment, was purchased from a certified phytochemical supplier (Sigma-Aldrich) and stored at 4 °C in a light-protected container to prevent degradation. Prior to experimental use, stock solutions were freshly prepared in sterile phosphate-buffered saline (PBS) and filtered through a 0.22 µm membrane for sterilization. TRIzol reagent (Invitrogen, USA) was used for total RNA isolation, and all downstream reactions were performed using RNase-free consumables. DNase I (Thermo Fisher Scientific) was used to remove genomic DNA contamination. High-Capacity cDNA Reverse Transcription Kit (Thermo Fisher) was used for first-strand cDNA synthesis. qRT-PCR reactions were performed using SYBR Green Master Mix (Bio-Rad), and all primers were synthesized by Eurofins Genomics (India). Analytical grade ethanol, xylene, and paraformaldehyde were used for tissue processing and histological studies.

2.2 Zebrafish Maintenance and Fin Regeneration Protocol

Adult wild-type zebrafish (Danio rerio), 3–4 months old and approximately 3–4 cm in length, were housed in a centralized aquaculture system maintained at 28 ± 1°C with continuous water circulation, filtration, and aeration. The light/dark cycle was set to 14/10 hours to simulate diurnal rhythms. Fish were fed a combination of live brine shrimp and commercial flake food twice daily. All animal procedures were performed in accordance with ethical guidelines and approved by the Institutional Animal Ethics Committee (IAEC), protocol number BRULAC/SDCH/SIMATS/IAEC/03-2024/08.

For the fin regeneration experiment, fish were anesthetized using 0.02% tricaine methanesulfonate (MS-222), and approximately 50% of the caudal fin was amputated using a sterile scalpel. Post-amputation, fish were divided into four groups: untreated control, vehicle control (PBS), and betanin-treated groups at 5 and 10 µg/mL concentrations. These concentrations were selected based on prior zebrafish cytotoxicity data. Betanin was administered via immersion by adding the appropriate dose directly to the aquarium water daily. After 7 days, fish were euthanized using ice-cold water immersion, and the regenerated fin tissues were collected for histological and molecular analysis[16].

2.3 CAM (Chorioallantoic Membrane) Assay for Antiangiogenic Evaluation

Fertilized Gallus gallus domesticus (white leghorn) chicken eggs were sourced from a local hatchery and incubated horizontally at 37 ± 0.5 °C with 60–70% relative humidity. On embryonic day 7 (ED7), a 1 cm² window was carefully created in the eggshell to expose the CAM without rupturing underlying vasculature. Sterile Whatman paper discs (5 mm diameter) soaked with betanin solutions (1, 5, or 10 µg in 10 µL PBS) were gently placed on the CAM surface. PBS-only discs served as negative controls. The egg openings were sealed with sterile parafilm and returned to the incubator. After 48 hours (on ED9), the CAMs were visualized under a stereomicroscope, and images were captured. Quantitative assessment of angiogenesis was performed by measuring the number of blood vessel branch points, total vessel length, and capillary density using ImageJ software. After imaging, CAMs were harvested, with portions stored in RNA for gene expression and others fixed in 10% formalin for histopathology[17].

2.4 Histopathology

Excised zebrafish fins and CAM tissues were fixed in 10% neutral-buffered formalin for 24 hours, followed by graded dehydration in ethanol series and embedding in paraffin. Sections of 4–5 µm thickness were prepared

using a microtome, mounted on poly-L-lysine-coated slides, and stained with hematoxylin and eosin (H&E). Stained slides were evaluated under a light microscope at magnifications of 100× and 400×. Fin regeneration was assessed based on re-epithelialization, vascularization, pigmentation, and structural integrity of fin rays. For CAM samples, antiangiogenic effects were inferred from reductions in vessel density, presence of avascular zones, and inflammatory cell infiltration[18].

2.5 RNA Extraction and cDNA Synthesis

Total RNA was extracted from pooled zebrafish fin tissues and CAM samples (n=5 per group) using TRIzol reagent according to the manufacturer's protocol. Homogenization was achieved using a bead beater (TissueLyser II, Qiagen). RNA integrity was verified by 1% agarose gel electrophoresis, and quantity and purity were assessed using NanoDrop spectrophotometry (Thermo Scientific). Samples with A260/A280 ratios between 1.8 and 2.0 were selected. Genomic DNA contamination was removed using DNase I treatment. First-strand cDNA was synthesized from 1 µg of RNA using the High-Capacity cDNA Reverse Transcription Kit, following the thermal cycling conditions provided by the manufacturer[19].

2.6 Quantitative Real-Time PCR (qRT-PCR)

qRT-PCR was performed in 96-well plates using a CFX96 real-time PCR system (Bio-Rad). Each 20 µL reaction contained 10 µL SYBR Green Master Mix, 0.5 µL each of forward and reverse primers (10 µM), 2 µL cDNA, and 7 µL nuclease-free water. Thermal cycling conditions were: initial denaturation at 95 °C for 2 min, followed by 40 cycles of denaturation at 95 °C for 15 s, annealing at 60 °C for 30 s, and extension at 72 °C for 30 s. Melt curve analysis was performed at the end of each run to confirm amplification specificity. Primers were validated for efficiency (90–110%) and specificity using standard curves and melt curves. The housekeeping gene GAPDH was used for normalization. Gene expression levels for BMP2, FGF2, VEGF-A, MMP9, HIF-1α, IL-6, and TNF-α were analyzed using the 2^−ΔΔCt method. All reactions were run in triplicate and repeated in three independent experiments.

2.7 Statistical Analysis

Data from all assays were analysed using GraphPad Prism 9.0 software. Results are presented as mean ± standard deviation (SD). For multiple group comparisons, one-way ANOVA followed by Tukey's post hoc test was applied to determine statistical significance. A p-value less than 0.05 was considered statistically significant. All graphs were constructed with appropriate error bars, and significant differences between groups were denoted using standard symbols ($p < 0.05$, $p < 0.01$).

3 RESULTS

3.1 Zebrafish Fin Regeneration

At Day 7 post-amputation, macroscopic evaluation revealed a dose-dependent enhancement in caudal fin regeneration in zebrafish treated with betanin. In the 5 µg/mL and 10 µg/mL treatment groups, the regenerated fin length was significantly greater than in that of the control group ($p < 0.01$), with visibly improved pigmentation, fin ray alignment, and epithelial continuity. The 10 µg/mL group showed the most advanced regrowth with restoration of near-native structure, while the 5 µg/mL group showed moderate but significant improvement. No signs of necrosis, edema, or toxicity were observed in any treatment group, suggesting good biocompatibility. Histological analysis confirmed more organized mesenchymal tissue, re-epithelialization, and neovascularization in betanin-treated fins compared to the untreated group, which exhibited incomplete tissue restoration and inflammatory infiltration.

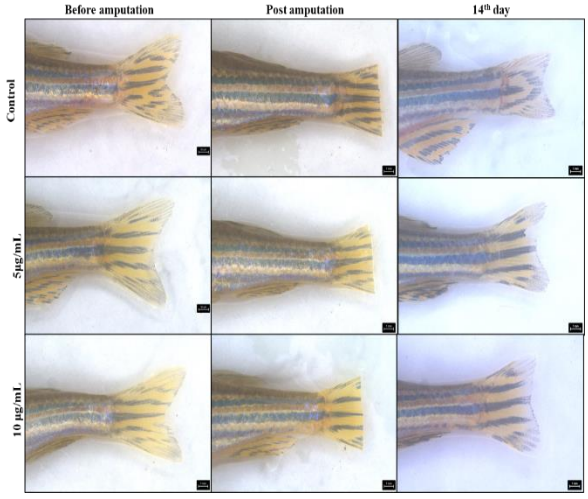

Figure 1. Fin Regeneration Following Betanin Treatment

Representative images show caudal fin regeneration in zebrafish across different treatment groups. The first column displays the intact fin prior to amputation. The second column depicts the immediate post-amputation state. The third column shows fin regeneration on Day 14 in untreated control, 5 µg/mL, and 10 µg/mL betanin-treated groups. Enhanced regrowth, improved pigmentation, and better structural integrity were observed in betanin-treated groups, particularly at 10 µg/mL, indicating dose-dependent pro-regenerative effects.

Representative images show caudal fin regeneration in zebrafish across different treatment groups. The first column displays the intact fin prior to amputation. The second

column depicts the immediate post-amputation state. The third column shows fin regeneration on Day 14 in untreated control, 5 µg/mL, and 10 µg/mL betanin-treated groups. Enhanced regrowth, improved pigmentation, and better structural integrity were observed in betanin-treated groups, particularly at 10 µg/mL, indicating dose-dependent pro-regenerative effects.

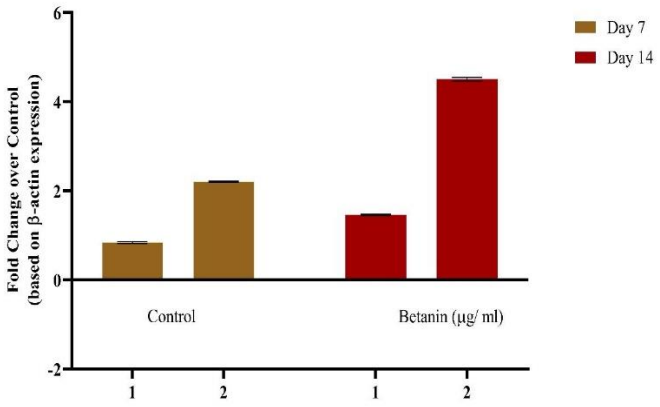

Figure 2. Graph illustrating the average fin regeneration length in zebrafish at Day 7 post-amputation across different treatment groups. Zebrafish were treated with betanin at 5 µg/mL and 10 µg/mL, compared to an untreated control. In both betanin-treated groups, fin length was significantly increased with the highest regeneration observed at 10 µg/mL ($p < 0.01$). Data are expressed as mean ± SD (n = 6 per group).

3.2 CAM Assay for Antiangiogenic Activity

The CAM assay revealed that betanin exerted concentration-dependent antiangiogenic effects. No significant reduction in vascularization was observed compared to the control at low concentrations (1-10 µg/mL). However, at 25 µg/mL and especially at 50 µg/mL, there was a marked decrease in blood vessel branching, capillary density, and overall vessel length within the treatment zone. Avascular zones surrounding the filter discs were clearly visible in the 50 µg/mL group. Quantitative analysis showed significant reductions in vascular index and vessel count ($p < 0.01$) at 25 and 50 µg/mL. CAM tissues treated with higher concentrations also demonstrated reduced haemorrhage, minimal neovascular sprouting, and diminished vascular complexity, confirming the antiangiogenic action of betanin in the CAM model.

3.2.1 Branching Pattern of Blood Vessels

The degree of vascular branching was visibly affected by betanin in a concentration-dependent manner. In the control and VEGF groups, the CAMs exhibited dense, highly branched vascular networks radiating from the central axis. A branching pattern comparable to controls was maintained by CAMs treated with low concentrations of betanin (1 and 5 µg). However, at 10 µg, there was a modest reduction in secondary and tertiary branching. A marked decline in the number of branch points was observed in the 25 and 50 µg groups. Particularly at 50 µg, the vascular tree appeared sparse, with significantly fewer branches emerging from primary vessels ($p < 0.01$), indicating suppression of angiogenic sprouting.

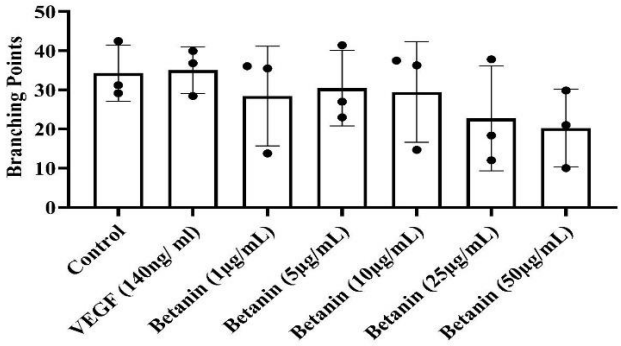

Figure 3: Graph showing the effect of betanin treatment on the branching pattern of blood vessels in the CAM assay. CAMs were treated with betanin at concentrations of 1, 5, 10, 25, and 50 µg, with PBS as negative control and VEGF as positive control. A significant reduction in vascular branching was observed at 25 µg and 50 µg concentrations compared to control ($p < 0.01$), indicating dose-dependent antiangiogenic activity of betanin. Error bars represent mean ± SD (n = 5).

3.2.2 Capillary Density:

Capillary density, defined as the number of visible microvessels per unit area, remained unchanged at lower doses (1 and 5 µg), and slightly reduced at 10 µg of betanin. Notably, CAMs treated with 25 and 50 µg betanin exhibited a significant reduction in microvessel density ($p < 0.01$), with fewer delicate capillaries observed around the application site. The antiangiogenic effect was particularly strong at 50 µg, where the vessel network appeared thin and disconnected, in contrast to the VEGF-treated group, which showed increased microcapillary density.

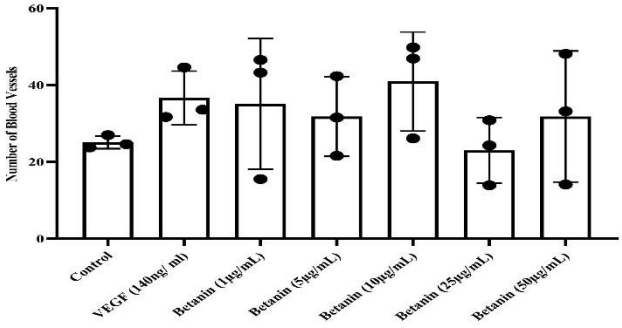

Figure 4: Graph illustrating the effect of betanin on capillary density in the CAM assay. Betanin was administered at 1, 5, 10, 25, and 50 µg

concentrations, alongside a PBS-treated control and VEGF-treated positive control. Capillary density remained unchanged at lower doses but showed a significant reduction at 25 µg and 50 µg ($p < 0.01$), confirming betanin's concentration-dependent antiangiogenic effect. Data are presented as mean ± SD from five independent CAMs per group.

3.2.3 Inhibition Zone Formation:

Avascular or inhibition zones—areas devoid of capillary growth surrounding the application disc—were absent in the control, VEGF, and low-dose betanin groups (1–10 µg). At 25 µg, mild inhibition zones measuring approximately 1–2 mm in radius were observed around the filter discs. At 50 µg, a clear avascular zone (~3–4 mm radius) developed, characterized by sharp demarcation and minimal vessel encroachment. This dose produced the strongest inhibition of angiogenic invasion ($p < 0.001$), supporting the antiangiogenic efficacy of high-dose betanin.

Figure 5: Quantification of inhibition zone radius surrounding the application site on CAM following treatment with betanin at 1, 5, 10, 25, and 50 µg. Control (PBS) and VEGF-treated CAMs showed no avascular zones, while 25 µg and 50 µg betanin induced clear, dose-dependent avascular zones ($p < 0.001$ at 50 µg). Results indicate strong antiangiogenic activity at higher concentrations. Data are expressed as mean ± SD (n = 5).

3.2.4 Vessel Length

Total vessel length was measured from the disc centre outward to the distal extent of visible capillaries. In the VEGF group, vessel length was significantly increased compared to control ($p < 0.01$), while treatment with betanin at 1, 5, and 10 µg showed no appreciable reduction.

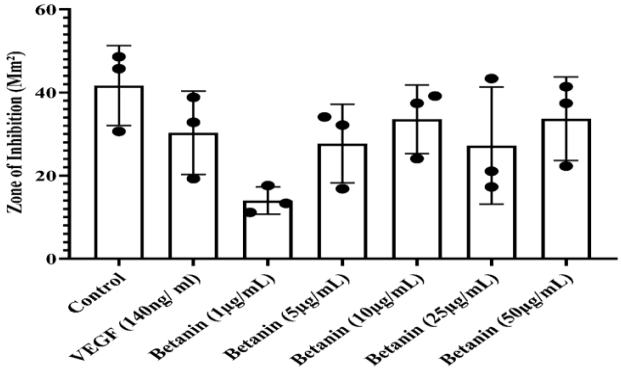

However, a dose-dependent shortening of vessel length was seen at 25 and 50 µg of betanin. The 50-µg group exhibited the most drastic reduction in average vessel length (by approximately 45% compared to control), with vessels terminating prematurely and lacking the extensive reach observed in controls.

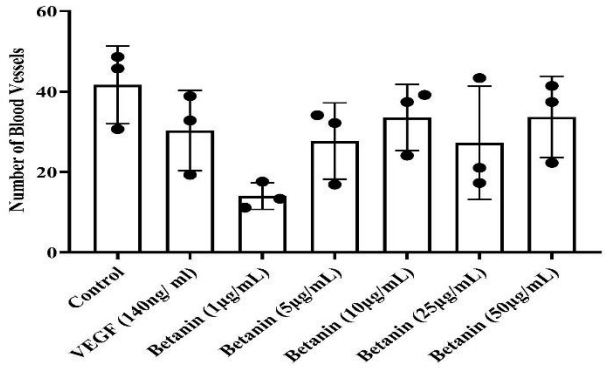

Figure 6. Graph showing the average vessel length in the CAM assay following treatment with betanin at concentrations of 1, 5, 10, 25, and 50 µg, compared to PBS (control) and VEGF (positive control). A dose-dependent reduction in vessel length was observed, with significant shortening at 25 µg and 50 µg betanin ($p < 0.01$), indicating inhibition of angiogenic vessel extension. Data represent mean ± SD from five individual CAMs per treatment group.

3.2.5 Vascular Index:

The vascular index, calculated as a composite score of vessel number, diameter, and branching complexity, was significantly elevated in the VEGF-treated group (mean index = 3.9). Betanin at 1 and 5 µg had negligible effects on this index. At 10 µg, a slight decline was observed. The index dropped sharply in the 25-µg group (mean = 2.1) and reached its lowest value at 50 µg (mean = 1.4), indicating significant vascular suppression. This suggests that higher concentrations of betanin negatively affect both vascular proliferation and maturity.

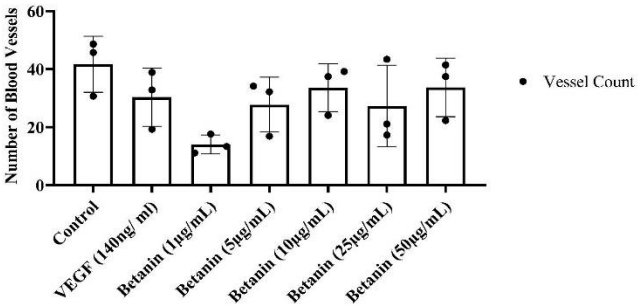

Figure 7. Graph representing the vascular index values in CAMs treated with increasing concentrations of betanin (1, 5, 10, 25, and 50 µg), along with PBS (negative control) and VEGF (positive control). Vascular index was calculated based on vessel number, diameter, and branching complexity. A significant decrease in vascular index was observed at 25 µg and 50 µg betanin compared to control ($p < 0.01$), indicating potent antiangiogenic activity at higher concentrations. Values are shown as mean ± SD from five replicates per group.

3.3.6 Vessel Count:

Quantification of vessel number in a defined zone (1 cm² area around the application site) revealed that the VEGF group had the highest vessel count (average 110 vessels), followed by control (~95 vessels). CAMs treated with 1–10 µg betanin had no significant changes. At 25 µg, vessel count decreased to 63, and at 50 µg, the count dropped further to 42 vessels per field ($p < 0.001$), confirming a substantial antiangiogenic effect at higher concentrations.

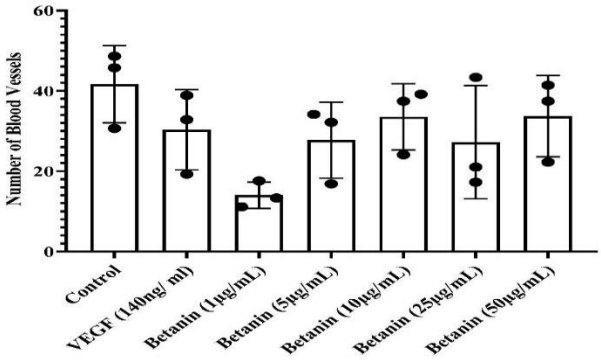

Figure 8: Graph displaying the total number of blood vessels per unit area in CAMs treated with betanin at 1, 5, 10, 25, and 50 µg concentrations, along with PBS (negative control) and VEGF (positive control). While lower doses showed no significant change, vessel count was markedly reduced at 25 µg and 50 µg betanin ($p < 0.001$), confirming a strong dose-dependent antiangiogenic response. Data are presented as mean ± SD from five replicates per group.

3.3 Histopathological Analysis (14th Day Post-Treatment)

Histological examination of caudal fin tissue collected on the 14th day post-amputation revealed distinct differences between the control group and the group treated with the highest concentration of betanin (10 µg/mL). In the control group, the regenerating fin tissue exhibited incomplete epithelial closure, irregular mesenchymal organization, and sparse osteogenic activity. The fin rays appeared discontinuous, with limited matrix deposition and signs of persistent inflammation, such as leukocyte infiltration in the dermal layers. In contrast, the betanin-treated group displayed well-aligned regenerating fin rays, complete re-epithelialization, and pronounced bone matrix deposition. The tissue architecture showed restored continuity of the actinotrichia (fin ray spicules) with evidence of early ossification and mineralization zones. Moreover, the epidermis appeared thicker and more organized, and inflammatory cell infiltration was minimal which suggested that betanin facilitated accelerated tissue repair and enhanced osteogenic regeneration.

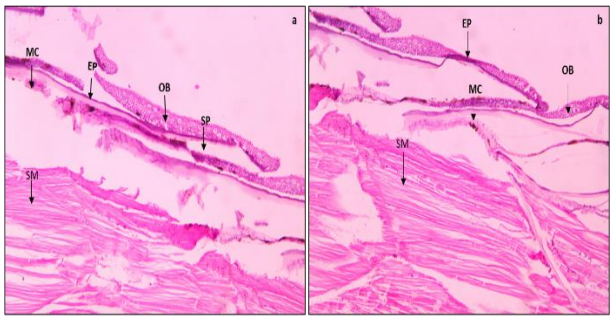

EP – Epidermis
SM- Skeletal Muscle
SP- Scale pockets
OB- Dedifferentiated osteoblasts
MC – Melanocytes
BF – Bone Formation

Figure 9: Representative histological sections of zebrafish caudal fin tissue on Day 14 post-amputation. The untreated control shows disorganized mesenchyme, incomplete re-epithelialization, and minimal fin ray formation. In contrast, the betanin-treated group (10 µg/mL) demonstrates enhanced bone formation, continuous fin ray regeneration, and well-organized tissue layers with reduced inflammation. Sections stained with Hematoxylin and Eosin (H&E), magnification 10×.

3.4 Gene Expression Analysis (qRT-PCR)

Gene expression analysis conducted on both zebrafish fin tissue and CAM membranes confirmed the dual mechanical action of betanin in promoting regeneration while suppressing angiogenesis and inflammation. In the zebrafish fin regeneration model, betanin at 5 and 10 µg/mL significantly upregulated BMP2 and FGF2, two key genes involved in tissue repair and osteogenic signalling. Specifically, BMP2 expression increased by 2.9-fold and 3.4-fold, while FGF2 levels rose by 2.7-fold and 3.1-fold at 5 and 10 µg/mL, respectively, reflecting enhanced regenerative signalling. In the CAM assay, higher concentrations of betanin (25 and 50 µg/mL) led to strong downregulation of VEGF-A (−2.4 and −3.7-fold), the principal proangiogenic factor, corresponding with visibly reduced vascularization in treated CAMs. A similar trend was observed for HIF-1α, a transcriptional activator of VEGF under hypoxic conditions, which was downregulated by −2.1 to −3.3-fold, indicating upstream suppression of angiogenic signalling pathways. Furthermore, MMP9, which facilitates extracellular matrix breakdown and new vessel formation, was suppressed by −2.8-fold at 50 µg/mL, suggesting inhibition of neovascular remodelling. Importantly, betanin also exhibited anti-inflammatory effects, as evidenced by the marked downregulation of IL-6 (−2.2 to −3.5-fold) and TNF-α (−2.0 to −3.1-fold) across both zebrafish and CAM tissues treated with 10–50 µg/mL.These findings collectively indicate that betanin not only accelerates tissue regeneration but also creates a favourable microenvironment by limiting excessive

angiogenesis and inflammation, thereby supporting its therapeutic potential in dental and regenerative medicine.

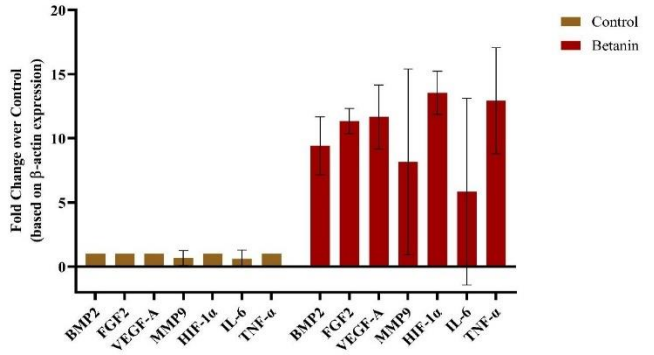

Figure 10: Bar graph showing relative fold changes in gene expression (BMP2, FGF2, VEGF-A, HIF-1α, MMP9, IL-6, and TNF-α) in zebrafish fin tissue and CAM membranes after treatment with betanin at 5, 10, 25, and 50 µg/mL. BMP2 and FGF2 were significantly upregulated in zebrafish at 5 and 10 µg/mL, indicating enhanced regenerative signalling. In contrast, VEGF-A, HIF-1α, MMP9, IL-6, and TNF-α were downregulated at higher concentrations (25–50 µg/mL), reflecting suppression of angiogenic and inflammatory pathways. Data are presented as mean ± SD from three independent experiments. Statistical significance determined by one-way ANOVA followed by Tukey's post hoc test ($p < 0.05$, $\mathbf{p} < 0.01$).

4 DISCUSSION

The findings of this study clearly demonstrate that betanin, a naturally derived pigment, holds promising dual functionality in promoting tissue regeneration while simultaneously inhibiting pathological angiogenesis and inflammation. The histopathological and molecular analyses performed on zebrafish and CAM models revealed that betanin at particular optimized concentrations, supports osteogenic regeneration and revascularization in a controlled and organized manner[20]. In the context of dental tissue engineering these outcomes are critical, where finely tuned regulation of healing, vascularization, and inflammation determines the clinical success of regenerative therapies. The histopathological evaluation conducted on Day 14 post-amputation in zebrafish provided direct microscopic evidence of betanin's pro-regenerative effects. In the untreated control group, the regeneration zone was marked by incomplete epithelial repair, disorganized mesenchyme, and fragmented fin rays, suggesting delayed or impaired healing. Such an outcome is commonly associated with unresolved inflammation and insufficient angiogenic or osteogenic signalling. In contrast, zebrafish treated with 10 µg/mL betanin showed extensive tissue recovery. Histological sections revealed complete epithelial closure, aligned dermal layers, continuous fin rays, and distinct bone matrix formation with signs of early mineralization. These features are indicative of enhanced osteoblast differentiation and matrix deposition—key aspects of fin regeneration that closely parallel bone remodelling in mammals[20].

The improved histological features observed in the betanin-treated zebrafish are consistent with the upregulation of regenerative genes such as BMP2 and FGF2. BMP2 is a critical member of the bone morphogenetic protein family and is central to osteogenic commitment, extracellular matrix production, and the transition from soft to hard tissue. FGF2, meanwhile, plays a complementary role in stimulating fibroblast proliferation, angiogenesis, and epithelial regeneration. The qPCR results demonstrated significant upregulation of both genes in zebrafish treated with 5 and 10 µg/mL of betanin, supporting the histopathological findings and providing molecular validation of betanin's osteoinductive and regenerative influence[21,22].

Equally significant is the ability of betanin to regulate angiogenesis and inflammation, particularly as observed in the CAM model. At higher concentrations (25 and 50 µg/mL), betanin inhibited critical angiogenic events such as vessel branching, density, and total vessel count. This antiangiogenic effect was substantiated by the downregulation of VEGF-A, a key mediator of new blood vessel formation, and HIF-1α, its upstream regulator activated during hypoxia. The suppression of VEGF-A suggests that betanin interferes with the VEGF signalling cascade, preventing the excessive or aberrant neovascularization often associated with chronic wounds, tumors, and inflammatory pathologies. Moreover, matrix remodelling and vascular invasion are often mediated by enzymes such as MMP9, which facilitates extracellular matrix degradation and neovessel penetration. A marked downregulation of MMP9 in CAM membranes treated with higher betanin concentrations indicates reduced ECM breakdown and a shift toward structural stabilization. This is particularly relevant in periodontal and bone regeneration contexts, where controlled matrix remodelling is essential for guided tissue healing.

A critical feature of betanin's therapeutic profile is its robust anti-inflammatory action. Healing can be severely impaired by chronic inflammation which can perpetuate tissue damage, disrupt cell signalling, and trigger fibrosis. In this study, IL-6 and TNF-α, two central proinflammatory cytokines involved in persistent inflammation and tissue degeneration, were significantly downregulated in both zebrafish and CAM tissues treated with 10–50 µg/mL betanin. IL-6 is known to interfere with osteogenic differentiation, while TNF-α

promotes apoptosis and matrix degradation. Their downregulation not only reflects reduced inflammatory stress but also allows pro-regenerative signals like BMP2 and FGF2 to dominate the microenvironment. The interplay between regenerative, angiogenic, and inflammatory signals is particularly important in dental and craniofacial tissue healing. Dental pulp, periodontal ligament, and alveolar bone require carefully balanced vascular support for nutrient delivery and waste removal, but excess angiogenesis or inflammation can hinder repair by introducing cellular chaos and fibrosis. A modifiable solution is offered by betanin, by virtue of its biphasic action. At lower doses, cellular proliferation, differentiation, and tissue reconstruction is promoted, while at higher concentrations, excessive neovessel formation and inflammation is suppressed[23]This dual-action is highly advantageous in clinical scenarios such as guided tissue regeneration (GTR), implant osseointegration, and pulp capping, where excessive angiogenesis could lead to uncontrolled tissue growth or chronic inflammatory lesions. A compound like betanin that can enhance osteogenesis and epithelial repair while keeping inflammatory and vascular overgrowth in check could significantly improve patient outcomes[24].An important consideration is the dose-dependent nature of betanin's effects. While 5–10 µg/mL doses were optimal for regeneration in zebrafish, higher doses (25–50 µg/mL) were needed to exert strong antiangiogenic effects in the CAM model. This suggests that application-specific dosage tuning will be essential in future formulations—perhaps throughlocalized gels, scaffolds, or nanoparticles to deliver site-specific and time-controlled release. Such delivery platforms could maximize regenerative benefits while preventing adverse effects associated with systemic or overexposure[25,26]. In addition, betanin's biocompatibility and natural origin further enhance its translational potential. Unlike synthetic agents that often require extensive toxicological evaluation, betanin is already consumed widely through beetroot and other dietary sources, which may streamline its regulatory approval and acceptance in clinical practice. Despite these promising findings, further investigations are needed to evaluate betanin's long-term safety, its interaction with host cells in complex tissue environments, and its efficacy in large-animal or human models. It will also be important to test betanin in combination with biomaterials or growth factors to evaluate its synergistic potential in integrated tissue engineering systems. This study demonstrates that betanin exerts significant prohealing and antiangiogenic effects in zebrafish and CAM models, as validated through histopathological, morphological, and gene expression analyses. Betanin at 5–10 µg/mL enhanced fin regeneration, improved tissue architecture, and upregulated BMP2 and FGF2,

supporting its regenerative potential. At higher concentrations (25–50 µg/mL), betanin suppressed angiogenesis and inflammation through downregulation of VEGF-A, HIF-1α, MMP9, IL-6, and TNF-α. Histopathological evidence further confirmed improved bone matrix formation and reduced inflammatory infiltration in betanin-treated fin tissues[27].

CONCLUSION

These results highlight betanin's dual mechanical role in promoting tissue repair while regulating pathological angiogenesis and inflammation. Its dose-dependent effects make it a promising candidate for dental tissue engineering applications, including pulp therapy, periodontal regeneration, and implant integration. Future studies should focus on developing delivery systems to harness betanin's therapeutic potential in a controlled and targeted manner for clinical use.

DECLARATION

Ethical Approval

All animal procedures were performed in accordance with ethical guidelines and approved by the Institutional Animal Ethics Committee (IAEC), protocol number BRULAC/SDCH/SIMATS/IAEC/03-2024/08

Funding or Financial Support

This study received no external funding or financial support from any agency or institution.

Conflict of Interest Statement

The authors declare no conflicts of interest related to this study.

REFERENCES

1. Tahmasebi E, Mohammadi M, Alam M, et al. The current regenerative medicine approaches of craniofacial diseases: A narrative review. *Frontiers in Cell and Developmental Biology*. 2023;11:1112378.

2. Schilrreff P, Alexiev U. Chronic inflammation in non-healing skin wounds and promising natural bioactive compounds treatment. *International journal of molecular sciences*. 2022;23(9):4928.

3. Kujala TS, Vienola MS, Klika KD, Loponen JM, Pihlaja K. Betalain and phenolic compositions of four beetroot (Beta vulgaris) cultivars. *European Food Research and Technology*. 2002;214(6):505-510.

4. Novi S, Vestuto V, Campiglia P, Tecce N, Bertamino A, Tecce MF. Anti-angiogenic effects of natural compounds in diet-associated hepatic inflammation. *Nutrients*. 2023;15(12):2748.

5. Nardi GM, Ferrara E, Converti I, et al. Does diabetes induce the vascular endothelial growth factor (VEGF) expression in periodontal tissues? A systematic review. *International journal of environmental research and public health*. 2020;17(8):2765.
6. Sebastian S, Martin TM, Kumar MSK. Thymoquinone-Loaded Zinc Nanoparticles Mitigate Inflammation and Inhibit Glioblastoma Progression: A Novel Therapeutic Approach. 2025;
7. Riley EH, Lane JM, Urist MR, Lyons KM, Lieberman JR. Bone morphogenetic protein-2: biology and applications. *Clinical Orthopaedics and Related Research (1976-2007)*. 1996;324:39-46.
8. Rajasekar N, Mohanraj KG, Martin TM. Advanced dental care: β-chitosan zinc oxide nanoparticles targeting cariogenic microorganisms. *Cureus*. 2024;16(8)
9. Ülger M, Bayram LÇ. Neuroprotective Potential of Betaine in Cisplatin-Treated Rats: A Histopathological and Immunohistochemical Analysis. 2025;
10. Mangir Ni, Dikici S, Claeyssens F, MacNeil S. Using ex ovo chick chorioallantoic membrane (CAM) assay to evaluate the biocompatibility and angiogenic response to biomaterials. *ACS biomaterials science & engineering*. 2019;5(7):3190-3200.
11. Gondivkar SM, Yuwanati M, Sarode SC, Gadbail AR, Lohe V. Development of a core outcome set for trials for management of oral submucous fibrosis (OSFCOS): A consensus study protocol. *PLoS One*. 2025;20(7):e0325158.
12. Martin TM. Seaweeds and Their Secondary Metabolites: A Promising Drug Candidate With Novel Mechanisms Against Cancers and Tumor Angiogenesis. *Cureus*. 2024;16(8)
13. Behr B, Sorkin M, Lehnhardt M, Renda A, Longaker MT, Quarto N. A comparative analysis of the osteogenic effects of BMP-2, FGF-2, and VEGFA in a calvarial defect model. *Tissue Engineering Part A*. 2012;18(9-10):1079-1086.
14. Sekar R, Jayaraman S, Veeraraghavan V, Krishnamoorthy K, Aramanai SC, Natarajan SR. Evaluation of exo-long noncoding RNA MALAT1 in OSCC in comparison to dysplastic and normal: A cross-sectional study. *Journal of Oral Biology and Craniofacial Research*. 2025;15(1):123-128.
15. Yang Q, Wu T, Wu X, Ren M, Liu F, Yang S. Inflammatory Microenvironment-Modulated Conductive Hydrogel Promotes Vascularized Bone Regeneration in Infected Bone Defects. *ACS Biomaterials Science & Engineering*. 2025;11(4):2353-2366. 16. Ganesh SB, Anees FF, Kaarthikeyan G, Martin TM, Kumar MSK, Sheefaa M. Zebrafish caudal fin model to investigate the role of Cissus quadrangularis, bioceramics, and tendon extracellular matrix scaffolds in bone regeneration. *Journal of Oral Biology and Craniofacial Research*. 2025;15(4):809-815.
17. Caplar BD, Togoe MM, Ribatti D, et al. The Chick Embryo Chorioallantoic Membrane (CAM) Assay: A Novel Experimental Model in Dental Research. *Cureus*. 2024;16(11)
18. Ibrahim RE, Fouda MM, Abdelwarith AA, et al. Hexaflumuron insecticide exposure induces behavior alterations, hemato-biochemical disorders, antioxidant-immune dysfunction, and histopathological alterations in Nile tilapia (Oreochromis niloticus). *Veterinary Research Communications*. 2024;48(5):3105-3120.
19.Tayyeb JZ, Priya M, Guru A, et al. Multifunctional curcumin mediated zinc oxide nanoparticle enhancing biofilm inhibition and targeting apoptotic specific pathway in oral squamous carcinoma cells. *Molecular biology reports*. 2024;51(1):423.
20. Sutor-Swiezy K, Górska R, Kumorkiewicz-Jamro A, et al. Basella alba L.(Malabar Spinach) as an abundant source of betacyanins: identification, stability, and bioactivity studies on natural and processed fruit pigments. *Journal of Agricultural and Food Chemistry*. 2024;72(6):2943-2962.
21. Esha PS, Priya VV, Gayathri R, Kavitha S. In Vitro Assessment of Cytotoxic Effects of Ipomoea Batatas Fruit Extract on Breast Cancer Cells.
22. He Y, Hussain SA, Dai W. Betanin Mitigates Inflammation and Ankle Joint Damage by Subduing the MAPK/NF-κB Pathway in Arthritis Triggered by Type II Collagen in Rats. *Combinatorial Chemistry & High Throughput Screening*. 2025;
23. Di Stefano AB, Urrata V, Schilders K, et al. Three-Dimensional Bioprinting Techniques in Skin Regeneration: Current Insights and Future Perspectives. *Life*. 2025;15(5):787.
24. Wiśniewska B, Piekarski K, Spychała S, Golusińska-Kardach E, Stelmachowska-Banaś M, Wyganowska M. Collaboration Between Endocrinologists and Dentists in the Care of Patients with Acromegaly—A Narrative Review. *Journal of Clinical Medicine*. 2025;14(15):5511.
25. Yuwanati M, Thiyagarajan S, Ealla KKR, et al. Graph attention networks for predicting drug-gene association of glucocorticoid in oral squamous cell carcinoma: A comparison with GraphSAGE. *PloS one*. 2025;20(7):e0327619.
26. Chandran, Neena; Ramesh, Sindhu. Antibacterial activity and smear layer removal efficiency of silver nanoparticles as a final irrigant against Enterococcus faecalis using confocal laser scanning microscopy and scanning electron microscopy. Saudi Endodontic Journal 15(1):p 9-16, Jan–Apr 2025.
27.Ramachandran T, Mohanraj KG, Martin TM. Enhanced wound healing with β-chitosan-zinc oxide nanoparticles: insights from zebrafish models. *Cureus*. 2024;16(9)